Adv Syst Sci Appl 2021; **02**:104–116
Published online at https://ijassa.ipu.ru.

Achieving Angular Superresolution of Control and Measurement Systems in Signal Processing

Boris Lagovsky[1], Evgeny Rubinovich[2*]

[1]*Russian Technological University (MIREA), Moscow, Russia*
[2]*Trapeznikov Institute of Control Sciences, Russian Academy of Sciences, Moscow, Russia*

Abstract: Algebraic methods of processing data obtained by control and measurement systems to achieve angular superresolution are presented. The efficiency of using the methods in the formation of approximate images of objects at low signal-to-noise ratios is shown. The results of numerical experiments demonstrate the possibility of obtaining images with a resolution exceeding the Rayleigh criterion by 3-10 times. The robustness of the solutions obtained by the methods of algebraic exceeds many well-known approaches. The relative simplicity of the presented methods allows the use of inexpensive computing devices and perform real-time measurement processing.

Keywords: angular superresolution, inverse problem, integral equation, Rayleigh criterion

1. INTRODUCTION

An important modern problem of improving control and measurement systems is increasing their information content based on new signal processing methods. One of the directions of its solution is to increase the angular resolution of angle-measuring systems, which makes it possible to detail the image of the object under study. In this regard, the problem of restoring the image of the object with an angular superresolution becomes highly significant. This paper is an extension of work in this direction originally presented in IEEE 2020 7th International Conference on Control, Decision and Information Technologies (CoDIT-2020) [1].

Due to the importance of the problem, hundreds of publications in many countries have already been devoted to the problems of achieving angular superresolution. We will highlight many articles that are general [2–5]. Currently popular methods are MUSIC [6–8], ESPRIT [9], the deconvolution method [10], the maximum entropy method [11, 12], the Borgiotti-Lagunas method [13], the Capon method [14], the maximum likelihood method [15] and others [16]. All these methods are not universal and are not always effective. They begin to work successfully and allow us to increase the effective angular resolution at a signal to noise ratio (SNR) not lower than 20-25 dB.

The developed algebraic methods [17–19] differ favorably from those mentioned above in that they have significantly higher noise immunity. In addition, they are relatively simple, which significantly reduces signal processing time and allows the use of relatively simple computing devices. As a result, unlike many other methods, it is possible to apply them in real-time.

*Corresponding author: rubinvch@hotmail.com

2. PROBLEM STATEMENT

Let us first consider the one-dimensional case. The signal $U(\alpha)$ received by the goniometer system when scanning the area under study is an integral transformation

$$U(\alpha) = \int_{\Omega} f(\alpha - \phi)\, I(\phi)\, d\phi, \tag{2.1}$$

where $f(\alpha)$ is the directional pattern (DP) of the system, $I(\alpha)$ is the unknown angular distribution of the amplitude of the signal reflected (or emitted) by the object, Ω is the angular sector, in which the object under study is located. The problem of reconstructing the image of the source $I(\alpha)$ with the highest possible angular resolution exceeding the Rayleigh criterion, i.e. with super-resolution, is posed. DP and measurement data in the form of $U(\alpha)$ are considered known.

Mathematically, the search for the angular distribution $I(\alpha)$ is reduced to the approximate solution of Fredholm integral equations of convolution type (2.1) concerning the function $I(\cdot)$.

It is known that of the three conditions for the correctness of Hadamard problems (existence of the solution, uniqueness of the solution, stability of the solution), the Fredholm equation (2.1) does not satisfy the second and third conditions. Thus, the problem under consideration belongs to the class of inverses and is incorrect. Because of this, attempts to increase the angular resolution and exceed the Rayleigh criterion generally lead to instabilities in the solutions and, as a result, to significant errors.

The main obstacle to obtaining solutions with super-resolution is the random components present in the received signal. When obtaining a resolution within the Rayleigh criterion, their influence is usually negligible but increases dramatically (exponentially) when trying to obtain a higher resolution. Achieving super-resolution, as studies show, is possible, but up to a certain limit, determined by the SNR, measurement accuracy, and accuracy of the DP assignment.

For a comparative assessment of the quality of the approximate solution of the problem (2.1), three indicators are usually used by different methods. The first one is the achieved degree of exceeding the Rayleigh criterion. The second indicator is the value of the displacement of the found positions of objects from the true ones since the positions of the resolved objects and their elements found during signal processing do not always exactly correspond to the actual directions to the radiation sources. When observing a single radiation source, the bias is usually close to zero. In the case of two or more sources, the offset can be different from zero and increase as you increase the reach of effective solutions.

The third indicator is the SNR, at which the specified degree of excess of the Rayleigh criterion is achieved. It is theoretically known and has been confirmed in the course of numerical experiments that the solutions of inverse problems are by their nature very sensitive *to the presence of random components in the source data*. Because of this, the first and third indicators can be combined. This is the dependence of the degree of excess of the Rayleigh criterion on the SNR. This indicator was considered the main one in the development of methods and algorithms for achieving superresolution.

3. ALGEBRAIC METHODS OF SOLUTION

To solve the inverse problem (2.1), we propose methods and algorithms for digital signal processing, which can be called algebraic. They consist in finding solutions in the form of decompositions over the given sequences of functions $g_m(\alpha)$ [20], which are orthonormal in

the region of the source location Ω.

$$I(\alpha) = \sum_{m=1}^{\infty} b_m g_m(\alpha) \cong \sum_{m=1}^{N} b_m g_m(\alpha), \tag{3.2}$$

where b_m are unknown expansion coefficients.

By using (3.2), instead of (2.1), we get a decomposition of the useful signal $U(\alpha)$ obtained by scanning over a system of non-orthogonal functions $\chi_m(\alpha)$

$$U(\alpha) \cong \sum_{m=1}^{N} b_m \chi_m(\alpha), \tag{3.3}$$

$$\chi_m(\alpha) \cong \int_{\Omega} f(\alpha - \phi)\, g_m(\phi)\, d\phi. \tag{3.4}$$

All the b_m necessary to obtain the solution (3.2) are found from the condition of minimizing the root-mean-square deviation of the right-hand side (3.3) from $U(\alpha)$. As a result, the search for the vector B of unknown coefficients b_m is reduced to the solution of SLAE:

$$V = GB, \tag{3.5}$$

where the elements of the vector V and matrix G are:

$$V_m = \int_{\Theta} U(\alpha)\chi_m(\alpha)\, d\alpha, \quad G_{nm} = \int_{\Theta} \chi_n(\alpha)\chi_m(\alpha)\, d\alpha, \tag{3.6}$$

$n, m = 1, 2, \ldots, N$.

Thus, the search for an approximate solution of $I(\alpha)$ in the form of a finite system expansion of the selected functions allows us to parametrize the inverse problem and reduce its solution to the SLAE solution [17–19].

The principal feature of the resulting systems is their ill-conditioned, which is a consequence of the attempt to solve the inverse problem. The larger the chosen area of integration Θ, the higher the stability of the obtained approximate solutions. However, the received signal always contains random components. For this reason, to obtain an adequate solution to the inverse problem (2.1), the level of the useful signal must significantly exceed the level of the random components. With the growth of Θ, the SNR decreases in the areas close to the boundary, which limits the area of integration Θ. Therefore, the integration region should be defined as the sector of angles within which the SNR value is sufficient to obtain stable solutions. It should be noted that the necessary SNR for obtaining solutions should be provided not directly at the reception of the signal but after the primary signal processing. So, the presented algebraic method and its variants make it possible, by consistently increasing the number of functions used in (3.2), i.e., by increasing the effective angular resolution, to approach the limit resolution for each problem to be solved. The iterative procedure for finding an approximate solution continues as long as it is possible to obtain a stable solution.

Comparing the algebraic method with others, it should be noted that it potentially allows one to obtain an exact solution to the inverse problem (2.1) if the chosen system of functions $g_m(\alpha)$ in (3.2) provides an exact representation of the solution $I(\alpha)$ using a finite number of terms. It is easy to prove that such a choice of the system $g_m(\alpha)$ for a known distribution $I(\alpha)$ is always possible. Thus, the algebraic method turns out to be at least as good as any other known method for solving the inverse problem (2.1). The question of choosing the optimal system of functions $g_m(\alpha)$ for the desired $I(\alpha)$ remains, however, open.

It is known that a significant improvement in the quality of solutions to inverse problems can be achieved by using a priori information about the solution. The presence of such

information allows, in particular, to use it when optimizing the choice of the system of functions $g_m(\alpha)$ for constructing a solution.

Preliminary information about the solution, in addition, is realized by using algebraic methods in the form of:

- choosing the location, size, and shape of the studied area of localization of the signal source Ω,
- introducing additional conditions in the form of equations and inequalities that connect the coefficients of expansion over sequences of functions and thereby regularize the problem.

Fig. 3.1 shows the solution to the problem of image reconstruction of two closely spaced smoothly inhomogeneous signal sources (dash line 1) in the form of a distribution of the reflected signal amplitude at a low noise level. For illustration, curve 3 shows a signal received by an angle-measuring system with a beamwidth of $\theta_{0.5}$ in the angular region of the source location. When constructing the solution (3.3)-(3.6), we used preliminary information

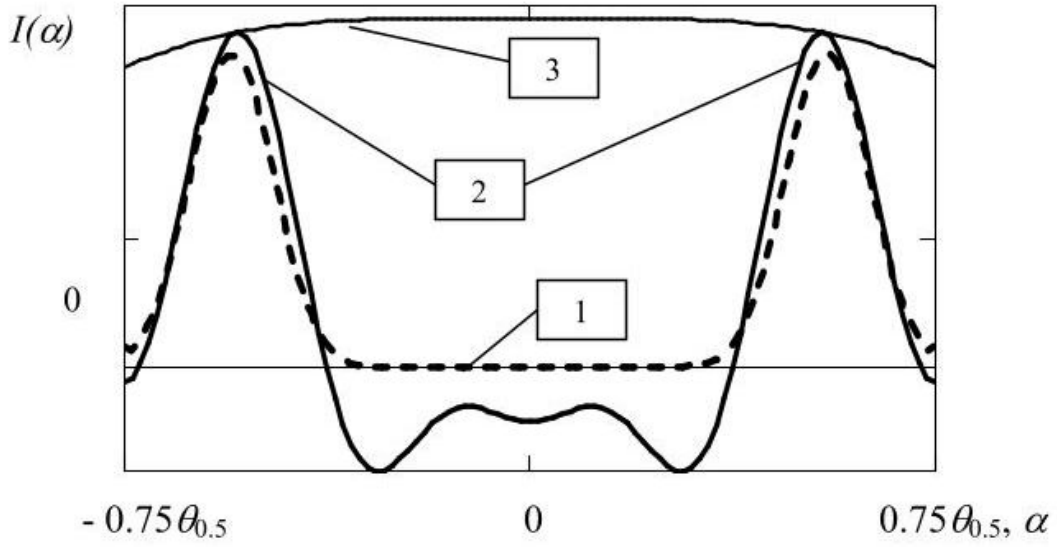

Fig. 3.1. The restoration of a smoothly inhomogeneous signal source

about the smoothly inhomogeneous nature of the amplitude angular distribution of the signal reflected by the source. This predestined the use of trigonometric functions as a system of functions $g_m(\alpha)$ in (3.2).

The resulting approximate solution (solid curve 2) allowed us to resolve the sources and almost accurately determine their angular position and shape. Due to the oscillating nature of the system of functions chosen to represent the solution, false sources with small amplitudes have emerged.

Fig. 3.2 shows the solution to the problem of image reconstruction of four closely located identical signal sources (dash line 1), close to the point at a very small SNR of 13 dB. The resulting approximate solution (solid line 2) allowed us to resolve all four sources and determine their angular position with good accuracy. For illustration, curve 3 shows the signal received and processed by the goniometer system. The usual methods of obtaining superresolution mentioned earlier do not allow us to obtain adequate solutions at such a low SNR level. Satisfactory solutions with the resolution of all four objects, but somewhat worse quality, can be obtained even at even lower SNR values.

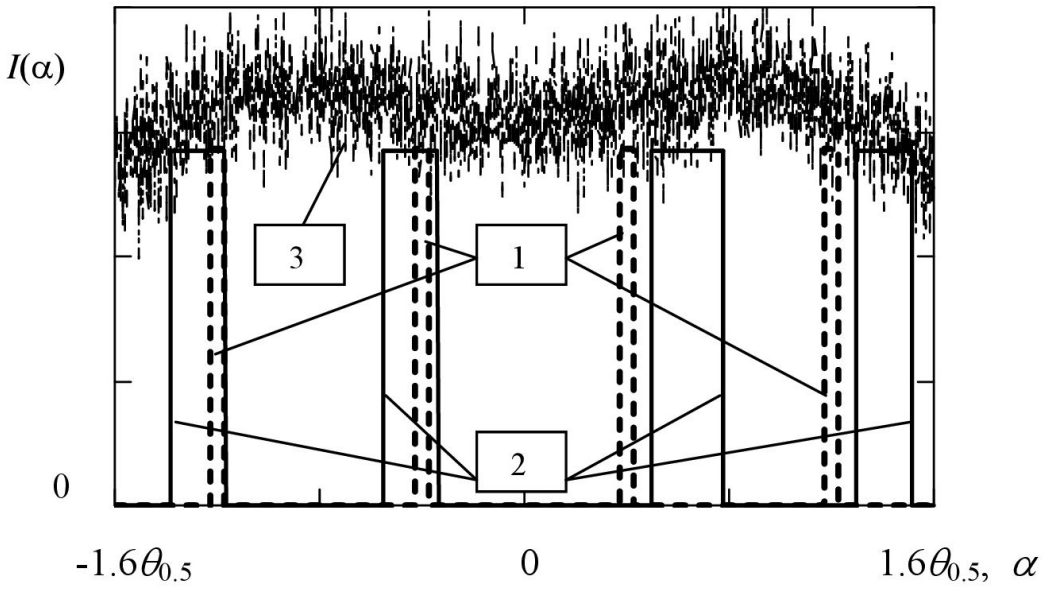

Fig. 3.2. The restoration of the images of point sources at low SNR

As already noted, with an increase in the number of functions $g_m(\alpha)$ used in the decomposition, the conditionality numbers of matrices G in (3.5) and similar ones, they increase sharply (according to the exponential law) and the solutions become less stable. The dimension of the matrices can be reduced by selecting the functions used. The purpose of selection is to select only those functions from the selected system that best represent the solution.

Selection can be carried out in several ways:

1. Based on the analysis of the signal spectrum and function spectra, followed by their selection with the spectra closest to the spectrum of the signal under study.

2. Based on the analysis of the mutual correlation functions of the signal and the functions from the selected family.

3. Based on the selection of functions from the used family with the highest values of the expansion coefficients in the solution representation.

Fig. 3.3 shows the results of restoring the source image at a very high noise level, comparable to the useful signal (SNR = 6-8 dB). The dashed curve is the original intensity distribution, the solid bold curve is the reconstructed image using six wavelets. For comparison, a solid thin polyline is shown as a reconstructed image using the same six wavelets in the absence of noise.

The obtained solutions provided a 2-3 fold excess of the Rayleigh criterion, and accuracy of source localization $\theta_{0.5}/8$, and very high noise immunity.

Most of the known methods are designed to obtain solutions to one-dimensional problems. Their generalization to two-dimensional problems significantly complicates the algorithms and increases the instability of solutions. In addition, the signal processing time increases dramatically. To obtain satisfactory results, it is sometimes necessary to use parallel processors. Generalization of algebraic methods for solving one-dimensional problems to two-dimensional ones does not lead to a serious complication of the algorithms.

We present the desired angular two-dimensional distribution $I(\alpha, \varphi)$ as a decomposition over a finite system of orthogonal functions $G_{nm}(\alpha, \varphi)$ in the two-dimensional domain Ω with

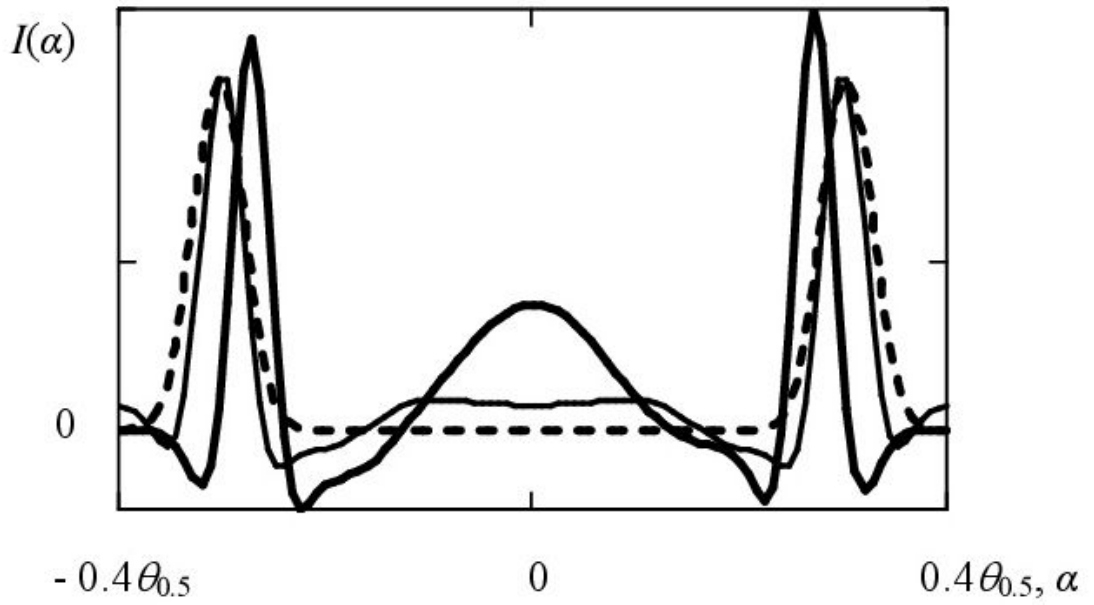

Fig. 3.3. Restoring the source image using the selected images MHAT wavelets at SNR = 6 dB

unknown coefficients. It is convenient to use separable systems, which are represented as the product of one-dimensional systems $G_{nm}(\alpha, \varphi) = g_n(\alpha)g_m(\varphi)$. Then:

$$I(\alpha, \varphi) \cong \sum_{n,m=1}^{N} b_{nm}\, g_n(\alpha)\, g_m(\varphi). \tag{3.7}$$

and the received signal by (2.1) is obtained in the form:

$$\begin{gathered} U(\alpha, \varphi) \cong \sum_{n,m=1}^{N} b_{nm}\, \Psi_{nm}(\alpha, \varphi), \\ \Psi_{nm}(\alpha, \varphi) = \int\limits_{\Omega} f(\alpha - \alpha',\, \varphi - \varphi')\, g_n(\alpha')\, g_m(\varphi')\, d\alpha'\, d\varphi', \\ n,\, m = 1, 2, \ldots, N. \end{gathered} \tag{3.8}$$

The coefficients b_{nm}, which provide the minimum root-mean-square deviation in the two-dimensional region Θ of the synthesized signal (3.8) from the received one, are found as SLAE solutions:

$$\begin{gathered} \int\limits_{\Theta} U(\alpha, \varphi)\, \Psi_{jk}(\alpha, \varphi)\, d\alpha\, d\varphi = \\ = \sum_{n,m=1}^{N} b_m \int\limits_{\Theta} \Psi_{jk}(\alpha, \varphi)\, \Psi_{nm}(\alpha, \varphi)\, d\alpha\, d\varphi, \\ j,\, k = 1, 2, \ldots, N. \end{gathered} \tag{3.9}$$

Numerical experiments have shown that the solution time and stability of solutions to two-dimensional problems in comparison with one-dimensional problems at the same level of

superresolution vary slightly [21, 22]. Thus, algebraic methods allow us to parametrize one- and two-dimensional inverse problems, and to reduce the solutions of integral equations to the SLAE solution, sometimes with additional conditions [23, 25, 27].

Fig. 3.4 shows an approximate solution of problems (3.7)-(3.9). The original source was defined as four identical objects with small angular coordinates, located at the corners of a square with a side of $0.9\theta_{0.5}$, which were not resolved by direct observation. The width $f(\alpha, \varphi)\theta_{0.5}$ was assumed to be the same at both corners.

When constructing the solution, we used preliminary information about the object under study as consisting of a group of small-sized sources. As $G_{nm}(\alpha, \varphi)$, functions close to Gauss functions were chosen to represent the solution, the maxima of which were located in the centers of squares with sides $\Delta\alpha$, $\Delta\varphi$ equal to $\theta_{0.5}/N$, into which the region was successively divided. The best solution with minimal errors was obtained at $N = 3$, i.e. when dividing the area Ω into 9 squares. Step $\Delta\alpha$ corresponded to the desired angular resolution.

As a result, all small-sized sources were resolved and their position was found with good accuracy. Since the inverse incorrect problem was solved, small errors appeared in the form of false sources with a small amplitude, which should be ignored when analyzing solutions.

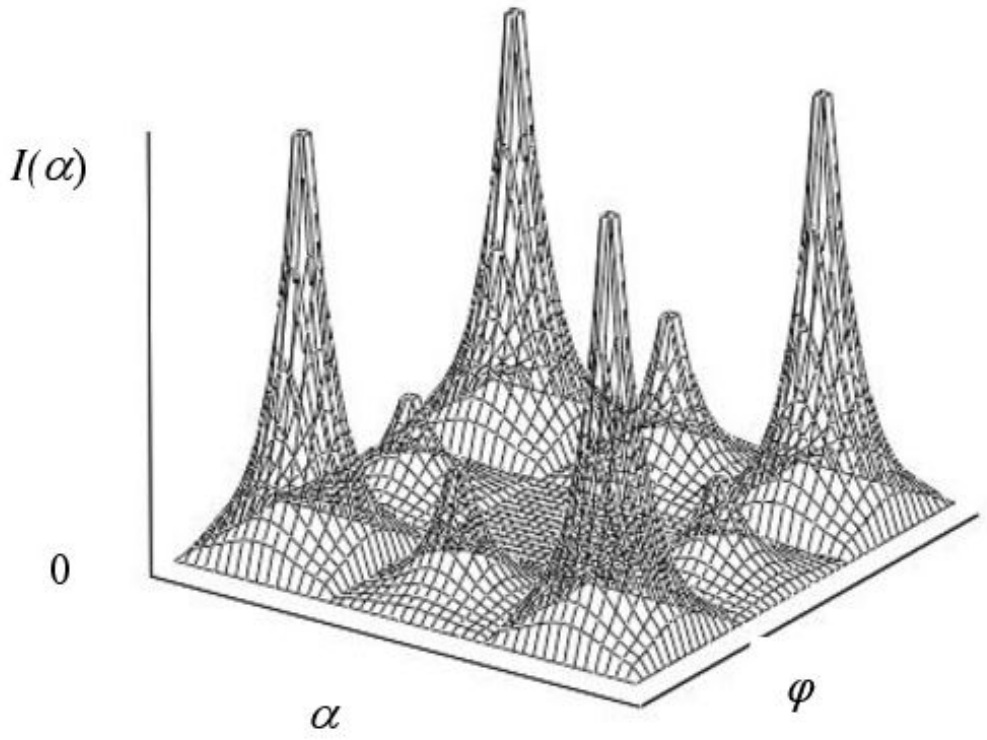

Fig. 3.4. Restored image of a two-dimensional source

4. TWO-BEAM METHOD

Further increase of the degree of achieved super-resolution is possible based of of more complex measuring and signal processing. In [24] considered the use of interpolation to find solutions with superresolution, in [19] described the use of regression methods for the analysis of measurement data in [28] using extrapolation methods, in [26] described the application of the developed technique in the use of UWB signals. Consider another possibility to increase the degree of superresolution when using active goniometer systems, i.e. systems that emit probing signals.

Let signal reception and radiation carried out by two independent scanning DP-transmitting $f_e(\beta)$ and receiving DP $f_r(\alpha)$. This, for example, can be achieved in the radio wave range using a smart antenna. Then, the relationship of the values I, U, and the scanning DP is expressed as the convolution integral of two variables α and β, which correspond to the positions of the maxima of the transmitting and receiving rays:

$$U(\alpha,\beta) = \int\limits_{\Omega} f_e(\alpha-\varphi)\, f_r(\beta-\varphi)\, I(\varphi)\, d\varphi. \tag{4.10}$$

The amount of information obtained by scanning with two beams (4.10) significantly exceeds the amount obtained by single-beam scanning (2.1). This allows us to expect to obtain a more accurate solution of the inverse problem (3.2)-(3.5) with a higher achievable level of superresolution.

One of the effective methods of signal processing (4.10) is the preliminary integration of the scanning angle β of the receiving or α emitting antenna. The larger the chosen area of integration Λ, the higher the stability of the obtained approximate solutions. However as Λ increases, the SNR decreases in areas close to the boundary. Therefore, the integration region should be defined as the sector of angles within which the SNR value is sufficient to obtain stable solutions. Usually, the area of Λ is noticeably larger than the area of Ω.

Integrating (4.10), for example, by the angle β we find

$$\begin{aligned} V(\alpha) &= \int\limits_{\Lambda} U(\alpha,\beta)\, d\beta = \\ &= \int\limits_{\Omega} f_e(\alpha-\varphi)\, I(\varphi) \int\limits_{\Lambda} f_r(\beta-\varphi)\, d\beta\, d\varphi = \\ &= \int\limits_{\Omega} f_e(\alpha-\varphi)\, I(\varphi)\, F(\varphi)\, d\varphi = \int\limits_{\Omega} f_e(\alpha-\varphi)\, \tilde{I}(\varphi)\, d\varphi, \end{aligned} \tag{4.11}$$

where

$$F(\varphi) = \int\limits_{\Lambda} f_r(\beta-\varphi)\, d\beta, \quad \tilde{I}(\varphi) = I(\varphi)\, F(\varphi). \tag{4.12}$$

The resulting integral equation (4.11) for the introduced function $\tilde{I}(\varphi)$ formally coincides with the original one (2.1). Therefore, processing of the results may be carried out using all techniques and algorithms applicable to (2.1). The solution (4.11) in the form of $\tilde{I}(\varphi)$ allows using (4.12) to easily express the desired distribution $I(\alpha)$.

Numerical studies on models have shown that the conditionality numbers of matrices of type (3.4)-(3.5) obtained for the problem (4.11) are significantly smaller than those of matrices G from (3.4). This indicates increased stability of the resulting solutions. In addition, pre-integration (4.11) reduces the role of random rapidly oscillating noise components of the signal, and thus also increases the stability of solutions. Increasing resiliency allows us to use more functions when presenting solutions (3.2) and, as a result, to get a higher resolution.

The disadvantage of pre-integration is the increased signal processing time. To increase the processing speed, instead of integrating by α and β, we can set a selection of angle values (α_p, β_q), $p, q = 1, 2, \ldots, N$, covering the entire scan area Λ. Then, instead of (4.11), using (3.2), we get

$$V(\alpha, \beta) = \sum_{m=1}^{N} b_m \int_{\Omega} f_e(\alpha_p - \varphi)\, f_r(\beta_q - \varphi)\, g_m(\varphi)\, d\varphi. \tag{4.13}$$

By entering the notation

$$\begin{aligned} W_{pq} &= U(\alpha_p, \beta_q), \\ \Phi_{pqm} &= \int_{\Omega} f_e(\alpha_p - \varphi)\, f_r(\beta_q - \varphi)\, g_m(\varphi)\, d\varphi, \end{aligned} \tag{4.14}$$

we arrive at the SLAE with respect to the coefficients b_m in the form

$$W_{pq} = \sum_{m=1}^{m} \Phi_{pqm}\, b_m, \quad p, q = 1, 2, \ldots, N. \tag{4.15}$$

The system (4.15) is overridden. Its solution is sought by standard algorithms in the root-mean-square approximation, which reduces the role of random components in the received signal.

The solutions of the system (4.15), as shown by numerical experiments on a mathematical model, are not inferior in stability to solutions based on integration (4.11),(4.12). At the same time, the signal processing speed based on (4.13)-(4.15)is noticeably higher, which allows the algorithm to be used in real-time.

Fig. 4.5 illustrates the differences in the quality of solutions to inverse problems by the one-and two-beam method with a low SNR of 11 dB. The true source of the reflected signal was two separate small-sized sources with a distance between them of $0.7\theta_{0.5}$, which were not resolved by direct observation (the solid curve 1). Step functions were chosen to represent the solution $I(\alpha)$. The solution based on the single-beam method is presented using the dashed curve 2. It should be considered inadequate: the image has little to do with the true sources. At the same time, the solution based on the two-beam method (the solid curve 3) allowed us to resolve the sources and correctly localize their location. The resulting false objects are characterized by a small amplitude of the reflected signal, and they should be ignored when solving such inverse problems.

Thus, the two-beam method of object image reconstruction reduces the role of random components, which ultimately manifests itself as an additional regularizing factor that increases the stability of solutions to the inverse problems under consideration. This is fully inherent in two-dimensional problems.

When scanning the two-dimensional region Θ with the transmitting and receiving beams at the angles (α, φ) and (γ, β), respectively, the received signal is obtained in the form:

$$\begin{aligned} U(\alpha, \varphi, \gamma, \beta) &\cong \sum_{n,m=1}^{N} b_{nm}\, \Psi_{nm}(\alpha, \varphi, \gamma, \beta), \\ \Psi_{nm}(\alpha, \varphi, \gamma, \beta) &= \\ &= \int_{\Omega} f_r(\alpha - \alpha', \varphi - \varphi') f_e(\gamma - \alpha', \beta - \varphi') g_n(\alpha') g_m(\varphi') d\alpha' d\varphi'. \end{aligned} \tag{4.16}$$

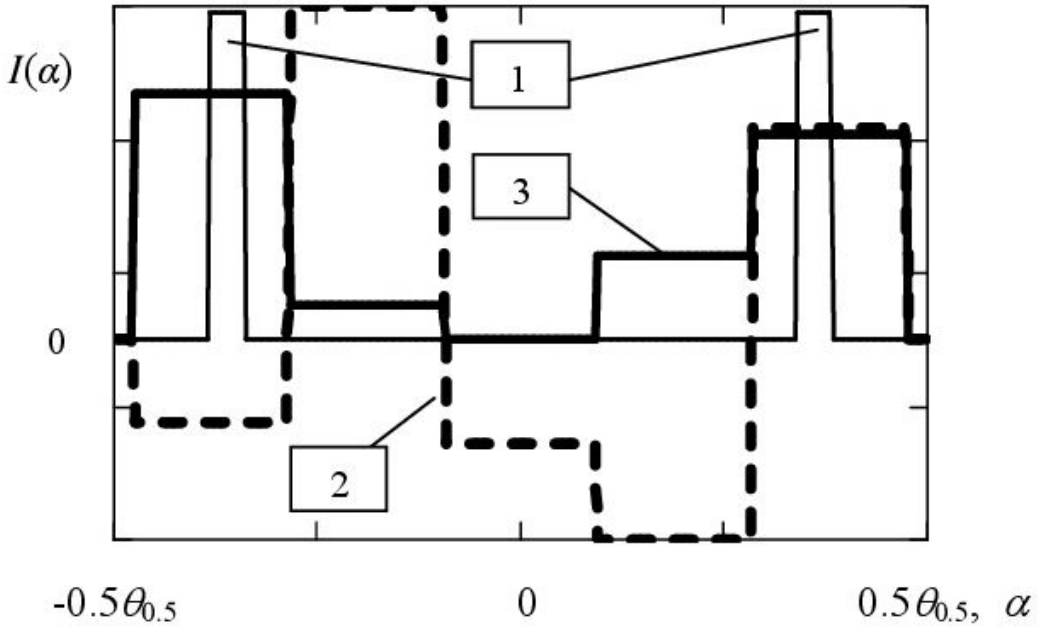

Fig. 4.5. Single - and double-beam solutions at high noise levels

Using the representation (3.7), the coefficients b_{nm}, which provide a minimum of the root-mean-square deviation of the sum in (4.16) from the received signal, are found as solutions of SLAE:

$$\int_{\Theta} U(\alpha,\varphi,\gamma,\beta)\,\Psi_{nm}(\alpha,\varphi,\gamma,\beta)\,d\alpha\,d\varphi\,d\gamma\,d\beta =$$

$$= \sum_{n,m=1}^{N} b_{nm} \int_{\Theta} \Psi_{jk}(\alpha,\varphi,\gamma,\beta)\,\Psi_{nm}(\alpha,\varphi,\gamma,\beta)\,d\alpha\,d\varphi\,d\gamma\,d\beta,$$

$$j,k = 1,\ldots,N.$$

To increase the processing speed, as previously for one-dimensional tasks, we can set a selection of angle values that cover the entire scan area instead of integrations.

Fig. 4.6,4.7 show the solution to the problem of restoring the image of a two-dimensional object. The rectangular coordinate system (α,φ) is used. A complex object consists of four identical small-sized objects located at the corners of a square with a side of $0.6\theta_{0.5}$. Fig. 4.6 shows their location in the Θ area. In the same figure, the $U(\alpha,\varphi)$ signal received during a single-beam scan is shown in the form of a grid. Direct observation, as well as the processing $U(\alpha,\varphi)$, did not allow us to obtain a stable solution in the form of an image of an object with a super-resolution. The use of a two-beam method of measurement and signal processing provided an image of the object. Fig. 4.7 shows the results of the mentioned signal processing in the region Ω when using step functions. The decision based on of a two-beam method has allowed us to resolve all four sources. Their angular position is correctly found and localized. The complex objects that arise when solving the inverse problem have a small amplitude and can be considered as angular noise. When solving problems of this kind, they should be filtered out, for example, using threshold devices.

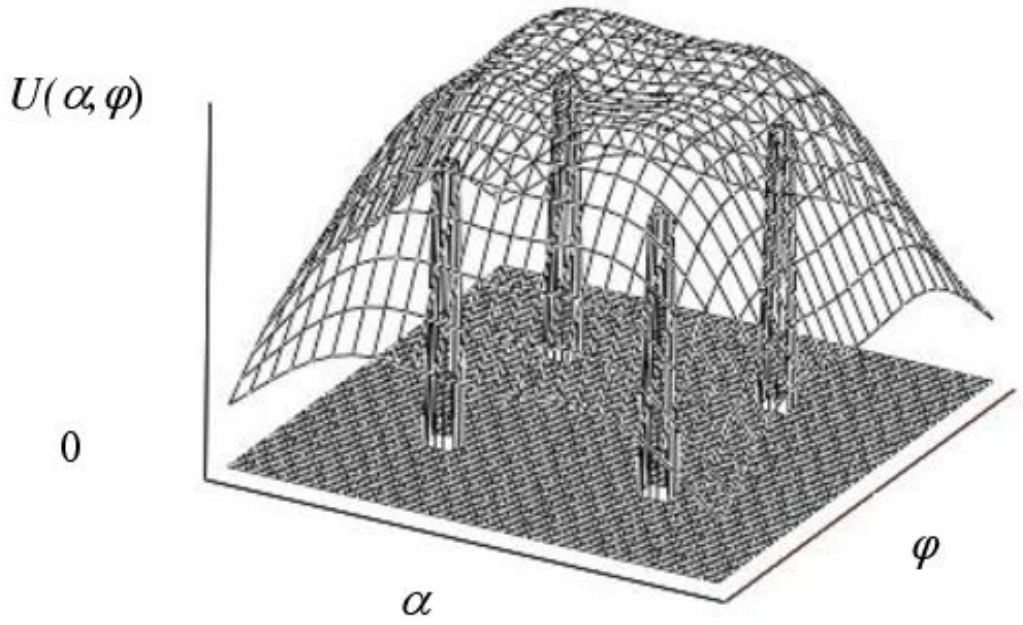

Fig. 4.6. The location of individual elements of a complex object and the angular distribution of the received signal

5. CONCLUSION

The developed algebraic methods of signal processing allow us to form approximate images of complex one-and two-dimensional objects with super-resolution. The achieved angular resolution increases when using a priori information about the solution reaches values 5-10 times higher than the Rayleigh criterion. Images are restored with relatively small errors in the values of the intensity and angular positions of individual elements of objects. The results of numerical studies have shown that the minimum required for obtaining a stable solution with a superresolution of SNR is 12-16 dB for simple algebraic methods, which is significantly less than for known methods. Modifications of algebraic methods based on two-beam scanning, targeted selection of functions chosen to represent the solution, and extensive use of a priori information about the solution allow us to obtain a stable solution with a superresolution in some cases up to an SNR of 7-9 dB. In an alternative interpretation, the modified algebraic methods of constant SNR allow increasing the level of the achieved superresolution. The created high-speed algorithms for algebraic methods allow to process of signals in a real-time mode.

Acknowledgment The reported study was partially supported by RFBR research project No. 20-07-00006.

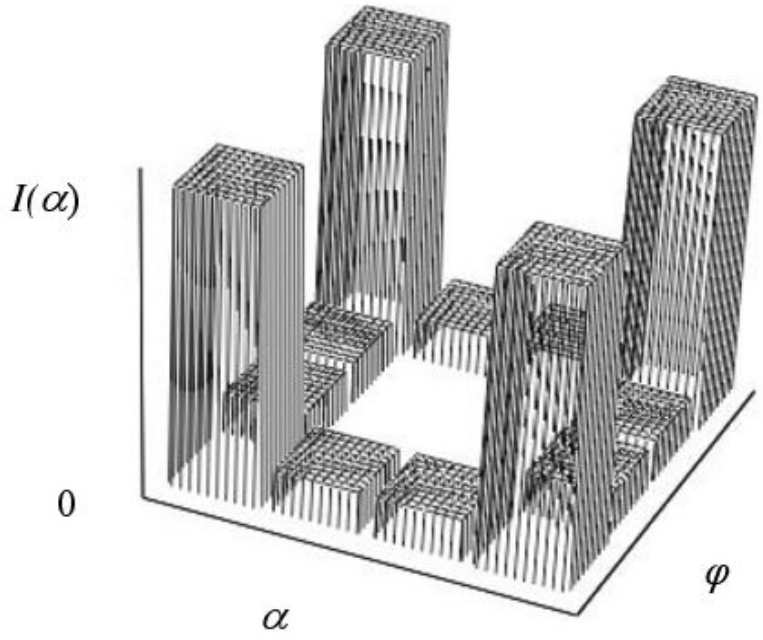

Fig. 4.7. Restored image of the object in Fig. 4.6

REFERENCES

1. Lagovsky B., Rubinovich E. (2020). Increasing the angular resolution of control and measurement systems in signal processing. *Proc. of the 7th Int. Conf. on Control, Decision and Information Technologies (CoDIT)*, 496–500.
2. Kasturiwala S., Ladhake S. (2010). Superresolution: a novel application to image restoration. *J. comput. sci. inf. technol*, (5), 1659–1664, .
3. Uttam S., Goodman N. (2010). Superresolution of coherent sources in real-beam data. *IEEE Trans. Aerosp. Electron. Syst.*, **46**(3), 1557–1566.
4. Park S., Park M., Kang M. (2003). Superresolution image reconstruction: a technical overview. *IEEE Signal Process. Mag.*, **20**(3), 21–36.
5. Kulikov N., Dung N. (2018). Analysis of noise immunity of reception of signals with multiple phase shift keying under the influence of scanning interference. *Russian technological journal.* **6**(6), 5–12.
6. Waweru N., Konditi D., Langat P. (2014). Performance analysis of music root-music and esprit doa estimation algorithm. *Int. J. Electr. Comput. Eng.*, **1**(8), 209–216.
7. Rao B., Hari K. (1989). Performance analysis of Root-Music. *IEEE Trans. Acoust.* **37**(12), 1939–1949.
8. Kim K., Seo D., Kim H. (2002). Ecient radar target recognition using the MUSIC algorithm and invariant features. *IEEE Trans. Antenn. Propag.* **50**(3), 325–337.
9. Lavate T., Kokate V., Sapkal A. (2010). Performance analysis of MUSIC and ESPRIT DOA estimation algorithms for adaptive array smart antenna in mobile communication. *Proc. of the 2nd Int. Conf. on Computer and Network Technology*. 308–311.
10. Almeida M., Figueiredo M. (2013). Deconvolving images with unknown boundaries using the alternating direction method of multipliers. *IEEE Trans. Image Process.* **22**(8), 3074–3086.

11. Guan J., Yang J., Huang Y., et. al. (2014). Angular superresolution algorithm based on maximum entropy for scanning radar imaging. *IEEE Int. Geoscience and Remote Sensing Symp.* 3057–3060.
12. Gamboa F., Gassiat E. (1996). Sets of Superresolution and the Maximum Entropy Method on the Mean. *SIAM J. Math. Anal.* **27**, 1129–1152.
13. Borgiotti G., Kaplan L. (1979). Superresolution of uncorrected interference sources by using adaptive array technique. *IEEE Trans. Antenn. Propag.* **27**(11), 842–845.
14. Capon J. (1969). High-resolution frequency-wavenumber spectrum analysis. *Proc. IEEE 1969*. **27**(1), 1408–1418, .
15. Stoica P., Sharman K. (1990). Maximum likelihood methods for direction-of-arrival estimation. *IEEE Trans. Acoust.* **38**(7), 1132–1143, .
16. Li L., Hurtado M., Feng X., et. al. (2018). A survey on the low-dimensional-model-based electromagnetic imaging. *Found. Trends Signal Process.* **12**(2), 107–199, .
17. Lagovsky B., Samokhin A., Shestopalov Y. (2016). Increasing effective angular resolution measuring systems based on antenna arrays. *Proc. 2016 URSI Int. Symp. Electromagnetic Theory (EMTS)*. 432–434, .
18. Lagovsky B., Chikina A. (2017). Superresolution in signal processing using a priori information. *PIERS Proc. Progress in Electromagnetics Research Symposium (PIERS 2017)*. 944–947.
19. Lagovsky B., Samokhin A., Shestopalov Y. (2019). Regression Methods of Obtaining Angular Superresolution. *Conference Paper 2019 URSI Asia-Pacific Radio Science Conference (AP-RASC).* 236–239.
20. Morse P., Feshbach H. (1953). *Methods of Theoretical Physics*. Science/Engineering/Math. NY: McGraw-Hill.
21. Lagovsky B., Samokhin A. (2013). Image Restoration of Two-dimensional Signal Sources with Superresolution. *PIERS Proc. Progress in Electromagnetics Research Symposium (PIERS 2013)*. 315–319.
22. Lagovsky B., Samokhin A., Shestopalov Y. (2018). Creating two-dimensional images of objects with high angular resolution. *IEEE Asia-Pacific Conf. on Antennas and Propagation (APCAP).* 114–115.
23. Lagovsky B. (2012). Superresolution: Data mining. *PIERS Proc. Progress in Electromagnetics Research Symp. (PIERS 2012-Moscow)*. 993–996.
24. Lagovsky B. (2012). Image Restoration of the Objects with Superresolution on the Basis of Spline - Interpolation. *PIERS Proc. Progress in Electromagnetics Research Symp. (PIERS 2012-Moscow)*. 989–992.
25. Lagovsky B. (2009). Algorithm for the determination of targets coordinates in structure of the multiple targets with the increased effective resolution. *PIERS Proc. Progress in Electromagnetics Research Symp. (PIERS 2009).* 1642–1645.
26. Lagovsky B., Samokhin A., Shestopalov Y. (2017). Increasing accuracy of angular measurements using UWB signals. *Proc. of the 11th European Conf. on Antennas and Propagation (EUCAP).* 1083–1086.
27. Lagovsky B., Samokhin A. (2017). Superresolution in signal processing using a priori information. *Proc. of the Int. Conf. Electromagnetics in Advanced Applications (ICEAA).* 779–783.
28. Lagovsky B., Samokhin A., Shestopalov Y. (2015). Superresolution Based on the Methods of Extrapolation. *PIERS Proc. Progress in Electromagnetics Research Symp. (PIERS 2015-Prague).* 1548–1551.

